RSC Advances

This is an *Accepted Manuscript*, which has been through the Royal Society of Chemistry peer review process and has been accepted for publication.

Accepted Manuscripts are published online shortly after acceptance, before technical editing, formatting and proof reading. Using this free service, authors can make their results available to the community, in citable form, before we publish the edited article. This *Accepted Manuscript* will be replaced by the edited, formatted and paginated article as soon as this is available.

You can find more information about *Accepted Manuscripts* in the **Information for Authors**.

Please note that technical editing may introduce minor changes to the text and/or graphics, which may alter content. The journal's standard **Terms & Conditions** and the **Ethical guidelines** still apply. In no event shall the Royal Society of Chemistry be held responsible for any errors or omissions in this *Accepted Manuscript* or any consequences arising from the use of any information it contains.

www.rsc.org/advances

Base-catalysed hydrolysis of PIM-1: amide versus carboxylate formation

Bekir Satilmis and Peter M. Budd

TABLE OF CONTENTS ENTRY

Controlled hydrolysis of PIM-1 yields polymers tailored for the selective adsorption of ionic dyes.

Journal Name
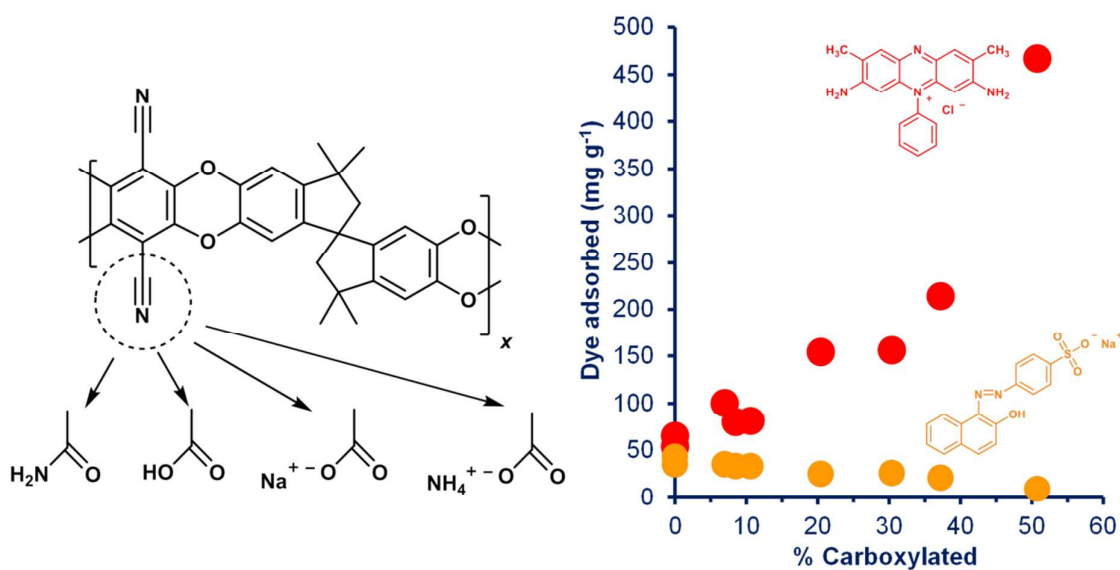
ARTICLE

Base-catalysed hydrolysis of PIM-1: amide versus carboxylate formation

Bekir Satilmis[a] and Peter M. Budd[a]*

Chemical modification can be used to tailor the properties of PIM-1, the prototypical polymer of intrinsic microporosity, which shows promise for applications such as membrane and adsorption processes for gas and liquid separations. Base-catalysed hydrolysis of PIM-1 has previously been assumed to yield only carboxylated products. In this work, hydrolysis was carried out at 120°C with 20% NaOH and at 100°C with 10% NaOH in a water/ethanol mixture, and a combination of IR, UV, ^{1}H NMR and elemental analysis was used to demonstrate that the hydrolysis products contain a mixture of amide, carboxylic acid, ammonium carboxylate and sodium carboxylate structures. The amide-PIM-1 structure has not previously been reported. Even the most fully hydrolysed samples had a substantial proportion of amide, with most samples being >50% amide. On hydrolysis there was a decrease in the water contact angle (from 85° for PIM-1 to about 60° for the most fully hydrolysed samples) and a decrease in the BET surface area. The adsorption of dyes from aqueous solution was shown to depend on the composition of the polymer. Uptake of the cationic dye Safranin O increased dramatically with increasing percentage carboxylation, the most highly carboxylated sample showing 31 times the uptake of the parent polymer, whereas uptake of the anionic dye Orange II decreased with increasing percentage carboxylation.

Introduction

Polymers of intrinsic microporosity (PIMs)[1, 2] behave as molecular sieves in the solid state because their contorted macromolecular backbones cannot fill space efficiently. PIMs have attracted attention as materials for membrane separations,[3-9] adsorbents,[10, 11] sensors,[12-14] catalysis[15, 16] and other applications. The prototypical solution-processable PIM, referred to as PIM-1 (**Fig. 1a),** is readily prepared by a double aromatic nucleophilic substitution reaction between two commercially available monomers (5,5',6,6'-tetrahydroxy-3,3,3',3'-tetramethyl-1,1'-spirobisindane and tetrafluoro-terephthalonitrile) and has been extensively studied. A variety of chemical modifications of PIM-1 have been reported, including conversion of the nitrile groups to carboxylic acid,[17-20] tetrazole,[21, 22] methyl tetrazole,[23] thioamide,[24] amidoxime[25, 26] and amine.[27] The sulfonation of PIM-1 has also been attempted,[28] and various approaches have been employed to crosslink PIM-1, including nitrene reactions with diazide

crosslinkers,[29, 30] as well as thermal treatment of the carboxylated polymer.[19]

Carboxylated PIM-1 has been reported as the product of base-catalysed hydrolysis of PIM-1.[17-20] For example, Du et al.[17] interpreted spectroscopy data for hydrolysed PIM-1 in terms of repeat units bearing zero, one or two nitrile groups, and correspondingly two, one or zero carboxylic acid groups. However, base-catalysed hydrolysis of a nitrile may potentially yield an amide as an intermediate product.[31, 32] For another nitrile-containing polymer, polyacrylonitrile, alkaline hydrolysis has been shown to yield products of complex chemical composition.[33-35] Here we demonstrate for PIM-1 that, by varying the reaction conditions and time, products may be generated with amide, carboxylic acid and carboxylate salts in various proportions. We further show that hydrolysis products differ in the adsorption of dyes from aqueous solution, uptake of the cationic dye Safranin O (**Fig. 1b**) increasing and uptake of the anionic dye Orange II (**Fig. 1c**) decreasing with increasing degree of carboxylation.
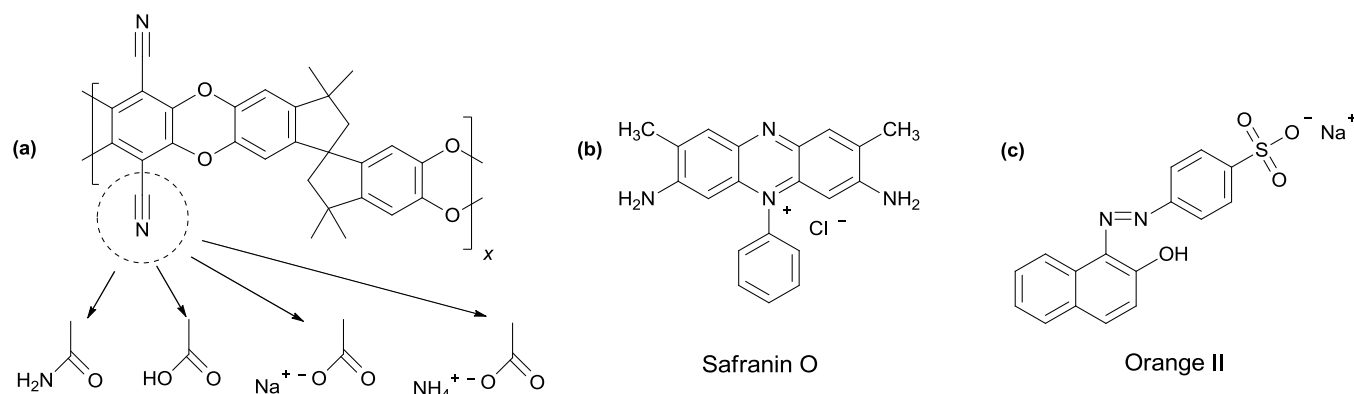
Fig. 1 Chemical structures of (a) the polymer of intrinsic microporosity PIM-1 and possible hydrolysis products, and dyes used in dye adsorption experiments: (b) Safranin O and (c) Orange II.

Experimental

Materials

Dimethylacetamide (DMAc), toluene, methanol (MeOH), sodium hydroxide, chloroform, Safranin O (>85% dye content) and Orange II sodium salt (>85% dye content) were purchased from Sigma-Aldrich and were used as received. Tetrafluoroterephthalonitrile (TFTPN, 98%, Aldrich) was purified by sublimation; it was heated to around 150 °C and the pure product collected without vacuum. 5,5',6,6'-Tetrahydroxy-3,3,3',3'-tetramethyl-1,1'-spirobisindane (TTSBI, 98%, Alfa Aesar) was dissolved in methanol and re-precipitated from dichloromethane before use. Anhydrous potassium carbonate (K$_2$CO$_3$, 99.0%, Fisher) was dried in an oven at 110 °C overnight before use.

Methods

Infrared (IR) spectra of powder samples were recorded on a Bio-Rad FTS 6000 spectrometer with an Attenuated Total Reflectance (ATR) accessory. Each sample was scanned 16 times at a resolution of 4 cm^{-1}. Peak areas were calculated using Omnic software.

Ultraviolet (UV) spectra were recorded on a Shimadzu UV-1800 spectrometer. Spectra over the wavelength range 200-800 nm were obtained for two different solvents: DMAc and DMSO. Polymer samples (~1 mg) were dissolved in solvent (10 mL). Solvent was used as a blank for baseline correction.

^{1}H nuclear magnetic resonance (NMR) spectra of the polymers were recorded using a Bruker DRX-400 MHz NMR spectrometer at room temperature or a Bruker AvanceII-500 spectrometer at elevated temperatures. Polymer solutions for NMR were prepared in CDCl$_3$ and/or deuterated dimethylsulfoxide (d$_6$-DMSO), left to stir overnight (when DMSO was used as solvent, the solution was heated to *ca.* 50 °C), then filtered into a 5 mm NMR tube through a small plug of glass wool in a Pasteur pipette, to filter out any residual solid particles. Signal peaks for solvents were used as references. When d$_6$-DMSO was used as solvent, measurements were carried out at 21.5°C, 50, 75, 100 and 120°C.

Elemental analysis was carried out by the School of Chemistry Microanalysis Service, University of Manchester.

Average molecular weights of the parent polymer were measured by multi-detector gel permeation chromatography (GPC). Analysis was performed in CHCl$_3$ at a flow rate of 1 mL min^{-1} using a Viscotek VE2001 GPC solvent/sample module with two PL Mixed B columns and a Viscotek TDA302 triple detector array (refractive index, light scattering, viscosity detectors). The data were analysed by the OmniSec program.

Thermogravimetric Analysis (TGA) was carried out using a Mettler Toledo Star System. Polymer samples were heated to 1000 °C at 10 °C min^{-1} under a nitrogen atmosphere.

Contact Angles were measured using a Krüss DSA 100 drop shape analyzer with deionized water. The drop needle diameter used was 0.56 mm and the machine dosing was set to S5 (M). The associated drop shape analysis program was used for computational analysis, with the drop type set to sessile and the drop subtype set to normal. The baseline for the contact angle measurements was manually detected. For contact angle measurements, thin films were prepared on glass microscope slides. PIM-1 (~0.01 g) was dissolved in 2 mL CHCl$_3$ and hydrolysed products (~0.01 g) were dissolved in 2 mL DMSO. They were dried at room temperature for approximately half an hour, then dried in a vacuum oven for 3 days at 110 °C.

N$_2$ adsorption isotherms at −196 °C were measured using a Micromeritics ASAP 2020 surface area and porosity analyser. A small amount of powdered sample (~0.1 g) was weighed into an analysis tube and degassed under high vacuum at 120 °C for 960 min. After reweighing the degassed sample, it was degassed again under high vacuum for a further 2 h to ensure all volatiles were removed before N$_2$ adsorption analysis. Samples were then degassed again for 2 h and a free space measurement carried out using helium. Brunauer-Emmet-Teller (BET) surface areas were calculated from N$_2$ adsorption isotherms by multi-point analysis.

For dye adsorption studies, aqueous stock solutions of Orange II sodium salt (molecular formula: C$_{16}$H$_{11}$N$_2$NaO$_4$S; molecular weight: 350.32) and Safranin O (molecular formula: C$_{20}$H$_{19}$ClN$_4$; molecular weight: 350.84) were prepared in deionized water. Different concentrations were prepared by dilution of the stock solutions with deionized water. Calibration solutions were prepared from 50 to 0.39 mg L^{-1} and their absorbances were measured using a Shimadzu UV-1800 spectrometer. Values of λ$_{max}$ for Orange II and Safranin O were taken as 484 and 509 nm, respectively. Specific absorption

coefficients, a, were determined as 0.0597 L mg^{-1} cm^{-1} for Orange II and 0.0893 L mg^{-1} cm^{-1} for Safranin O. An exact amount of oven-dried adsorbent (~10.0 mg) was placed in 50 mL of 50 ppm dye solution. The dye solution (pH ~ 6.4) containing the adsorbent was stirred well with a magnetic stirrer for 24 h, after which time there was little further uptake of dye. 3 mL aliquots were taken periodically by syringe and filtered through a PTFE hydrophobic filter (0.45 μm). The mass of dye adsorbed by the polymer, q_e (mg g^{-1}), was determined from the absorbance of the dye solution before contact with polymer, A_0, and the absorbance of the dye solution after reaching effective equilibrium with the polymer, A_e, using Eqn. (1).

$$q_e = \frac{(A_0 - A_e)V}{alm} \qquad (1)$$

where V is the total volume of dye solution, l is the path length in the spectrometer and m is the total mass of polymer.

Synthesis of PIM-1

TTSBI (34.04 g, 0.1 mol), TFTPN (20.01 g, 0.1 mol), anhydrous K$_2$CO$_3$ (41.4 g, 0.3 mol), DMAc (200 mL) and toluene (100 mL) were added under a nitrogen atmosphere to a dry 1 L three-necked round bottom flask equipped with a Dean-Stark trap and mechanical stirrer, in an oil bath pre-heated to 160 °C, and the reaction carried out for 40 min under reflux. At the end of the reaction, when stirring was stopped, the highly viscous solution formed a gel-like suspension, and around 30 mL of liquid had collected in the Dean-Stark trap. The crude polymer was dissolved in chloroform and re-precipitated from methanol. The product was refluxed for 12 h in deionized water and then dried at 110 °C for two days. Yield: 42 g (91 %). GPC: M_n = 30,000, M_w = 100,000, M_w/M_n = 3.3. ^{1}H-NMR (400 MHz, CDCl$_3$, δ, ppm): 6.75 (2H, s), 6.35 (2H, s), 2.26-2.09 (4H, dd), 1.40-1.10 (broad, 12H). ATR-IR (cm^{-1}): 2995, 2864, 2239, 1605, 1446, 1264. Anal. calcd for C$_{29}$H$_{20}$N$_2$O$_4$ (wt%): C: 75.64, H: 4.37, N: 6.08 Found: C: 73.62, H: 4.44, N: 5.96.

Hydrolysis of PIM-1

Hydrolysis was carried out by two different methods,

Method A (ACD samples): Dry PIM-1 powder (2.01 g) and 20% NaOH solution (H$_2$O/Ethanol = 1/1) were added to a two-neck round-bottom flask equipped with a rubber septum and condenser. The mixture was heated to 120 °C and left to stir at this temperature under reflux. Samples were taken periodically by syringe and the solid collected by vacuum filtration. Polymer samples were soaked in water (pH adjusted to ~4-5 by addition of a few drops of HCl) and boiled for 2 h. They were collected by vacuum filtration, then washed with water until it was neutral. A variation of this method was used for sample ACD23, which, after reaction, was refluxed in acidic water for 8 h, filtered under vacuum, then stirred in water for 4 h, filtered, and washed with water (~500 mL).

Method B (AMD Samples): The same procedure was followed with 10% NaOH solution (H$_2$O/Ethanol = 1/1) at 100 °C.

The reaction times of the samples are given in **Table 1**. For reaction times up to 8 h, the polymer remained as a powder in suspension. For the ACD series, after 14 h reaction, the particles appeared swollen.

Table 1 Temperatures and times of hydrolysis reactions

Sample	Reaction temp. (°C)	Reaction time (h)
ACD1	120	1
ACD8	120	8
ACD14	120	14
ACD21	120	21
ACD23	120	43
AMD1	100	1.5
AMD2	100	3
AMD3	100	4.5
AMD7	100	7

Results and discussion

Solubility

Whereas the parent polymer, PIM-1, is soluble in solvents such as chloroform and tetrahydrofuran, the hydrolysed products showed solubility in dimethylformamide (DMF), dimethylacetamide (DMAc) and dimethylsulfoxide (DMSO). Samples hydrolysed at 120°C with 20% NaOH (ACD series) were readily soluble at room temperature. Samples hydrolysed at 100°C with 10% NaOH (AMD series) required gentle heating to dissolve. Sample AMD1, from reaction for only 1.5 h at the lower temperature, was only partially soluble. Similarly, AMD2 (3 h reaction) exhibited some difficulty in dissolution.

Characterization of hydrolysis products

IR spectra of the parent PIM-1 and representative hydrolysis products are shown in **Fig. 2a**. The PIM-1 spectrum shows characteristic nitrile (2240 cm^{-1}) and ether stretches (1265 cm^{-1}). In addition, aliphatic and aromatic C-H stretches can be seen in the region 2800–3010 cm^{-1}. In the hydrolysed products, the nitrile absorption is diminished or lost, and new bands appear in the region 3000-3500 cm^{-1}. Bands in this region have previously been attributed to O-H stretches of a carboxylated polymer.[17] However, they may equally be attributed to N-H stretches of an amide. Similarly, strong carbonyl bands at 1600 and 1670 cm^{-1} may arise either from hydrogen-bonded carboxylic acid or from amide. Thus, infrared spectroscopy alone cannot distinguish between amide and carboxylic acid products. However, the ratio of intensities of the C≡N to C-H peaks, I_{CN}/I_{CH}, values of which are given in **Table 2**, can be used to calculate the extent of hydrolysis (see below). For hydrolysis at 120 °C with 20% NaOH, the nitrile absorption is almost entirely lost after 1 h (**Fig. 2a,** sample ACD1). For hydrolysis at 100 °C with 10% NaOH, the nitrile absorption continues to reduce over a 7 h period (**Fig. 2b**).

Journal Name   RSC**Publishing**

ARTICLE
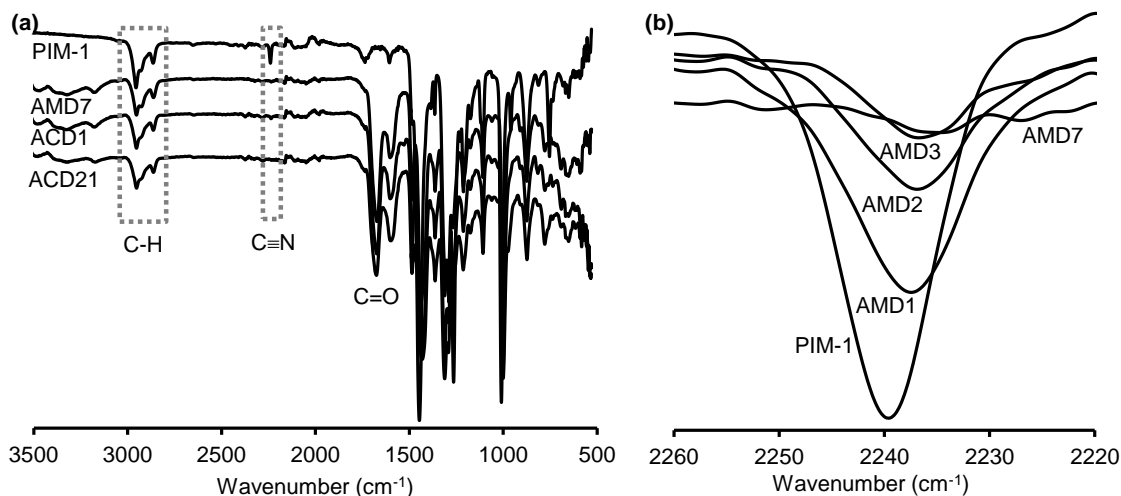
Fig. 2 (a) IR spectra of PIM-1 (top) and hydrolysis products AMD7, ACD1 and ACD21. (b) Nitrile region of IR spectra for PIM-1 and samples obtained after hydrolysis at 100°C with 10% NaOH for 1.5 h (AMD1), 3 h (AMD2), 4.5 h (AMD3) and 7 h (AMD7).

Table 2 Data from IR, UV and ^{1}H NMR spectroscopy, and elemental analysis of hydrolysed products.

Sample	IR I_{CN}/I_{CH}	UV absorbance in DMSO			UV absorbance in DMAc			^{1}H NMR I_{CO-H}/I_{Ar-H}	Elemental Analysis (wt.%)			
		326 nm	384 nm	444 nm	326 nm	384 nm	444 nm		C	H	N	Na
ACD1	0.0112	0.66	0.17	0	1.28	0.31	0.02	0.78	66.4	5.1	5.2	<0.3
ACD8	0.0065	1.26	0.06	0	1.19	0.05	0	0.77	65.4	5.2	4.5	<0.3
ACD14	0.0053	1.25	0.08	0	0.82	0.05	0	0.71	67.7	5.2	4.4	<0.3
ACD21	0.0024	0.68	0.02	0	1.01	0.04	0	0.61	65.7	5.1	4.2	1.6
ACD23	0.0011	1.05	0.03	0	1.53	0.03	0.01	0.50	61.5	4.4	2.8	3.2
AMD1	0.0517	0.37	0.7	0.22	0.49	0.91	0.28	0.47	70.3	5.4	5.4	<0.3
AMD2	0.0284	0.99	0.82	0.1	0.66	0.51	0.07	0.60	68.8	5.4	5.3	<0.3
AMD3	0.0165	0.83	0.32	0.03	0.46	0.16	0.01	0.71	68.1	5.1	5.1	<0.3
AMD7	0.0077	1.08	0.13	0	1.53	0.18	0.02	0.81	68.0	5.4	5.1	<0.3
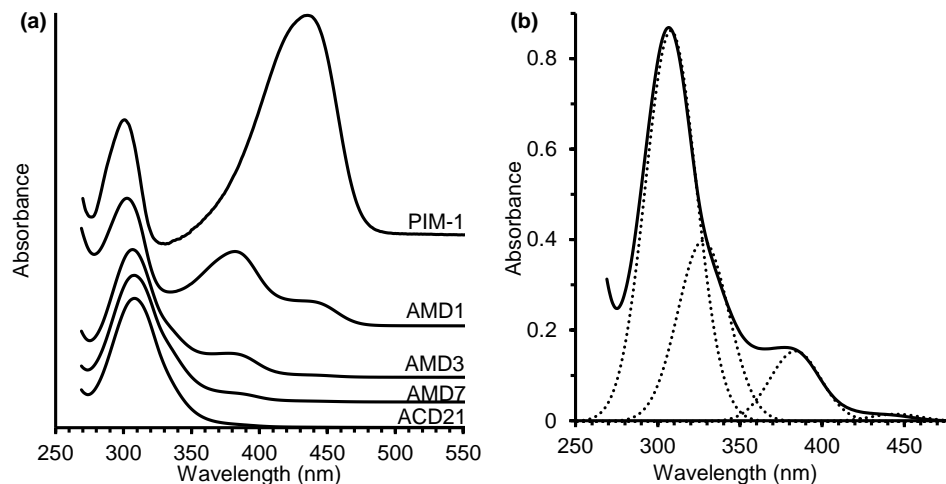
Fig. 3 (a) UV spectrum of PIM-1 and representative hydrolysis products in DMAc. Only low molar mass PIM-1 is soluble in DMAc, but the spectrum for high molar mass PIM-1 in CHCl$_3$ is similar. (b) Deconvolution of UV spectrum of sample AMD3 showing underlying peaks.

RSC Advances Accepted Manuscript

Journal Name

ARTICLE

UV spectra of PIM-1 and representative hydrolysis products are shown in **Fig. 3**. The UV spectrum of the parent polymer (PIM-1) shows two peaks with λ_{max} values in the region of 300 and 440 nm. The UV spectra of the most fully hydrolysed samples may be interpreted in terms of two overlapping peaks with λ_{max} values of 304 and 326 nm, and with no significant absorption beyond 380 nm. The UV spectra of partially hydrolysed samples may be interpreted in terms of four peaks with λ_{max} values of 304, 326, 384 and 444 nm (**Fig. 3b**). Values of absorbance at these wavelengths, for hydrolysed products in two different solvents (DMSO and DMAc) are included in **Table 2**. A repeat unit within the polymer may bear two nitrile groups (unconverted), one nitrile group (one converted to amide, carboxylate or carboxylic acid) or no nitrile groups (both converted). With increasing time of the hydrolysis reaction, the relative intensity of the peak at 444 nm diminishes, while the overlapping peak at 384 nm appears and then diminishes. The peaks at 384 and 444 nm may be assigned to unconverted nitrile, while the absorption which develops at 326 nm may be attributed to converted species. The relative intensities of these peaks may therefore be used to provide an alternative indication of the extent of hydrolysis (see below).

^{1}H NMR spectra of the parent PIM-1 and hydrolysis product ACD21 are shown in **Fig. 4**, with peak assignments for PIM-1, amide and carboxylic acid structures. For PIM-1 (in CDCl$_3$) four different proton environments can be seen. The aliphatic (0.9 to 2.5 ppm: H-1, H-2) to aromatic (6-7 ppm: H-3, H-4) peak intensity ratio is 4 (16H:4H). For the hydrolysed product

(in d$_6$-DMSO) additional peaks appear in the region 7−8 ppm, which may have contributions from amide and/or carboxylic acid protons. These peaks disappeared on addition of D$_2$O, but this does not distinguish between amide and carboxylic acid. Information about the composition can be obtained from the carbonyl:aromatic peak intensity ratio, which is 1 (4H:4H) for the fully amide structure and 0.5 (2H:4H) for the fully carboxylic acid structure. However, the ratio will also be 0.5 for a sample that is only half converted from nitrile to amide. Furthermore, because of difficulty in washing the hydrophobic polymer, carboxylate salts may not be fully converted to the acid form, and the presence of sodium or ammonium carboxylate will affect the results, as discussed further below. Values of carbonyl:aromatic peak intensity ratio, I_{CO-H}/I_{Ar-H}, determined at 120°C to reduce the influence of water in the solvent, are listed in **Table 2**. The samples with the lowest extents of hydrolysis (AMD1 and AMD2) were not fully soluble in DMSO, and the values of I_{CO-H}/I_{Ar-H} are therefore not representative of the sample as a whole. As discussed below, the ratio I_{CO-H}/I_{Ar-H} was used in combination with results from IR spectroscopy and elemental analysis to determine the composition of the hydrolysis products.

C, H, N and Na analysis results are included in **Table 2**. Samples were also analysed for chloride, but none was detected. Only samples ACD21 and ACD23 showed substantial sodium content, which was assumed to be as sodium carboxylate, the possibility of NaCl being ruled out by the absence of chloride.
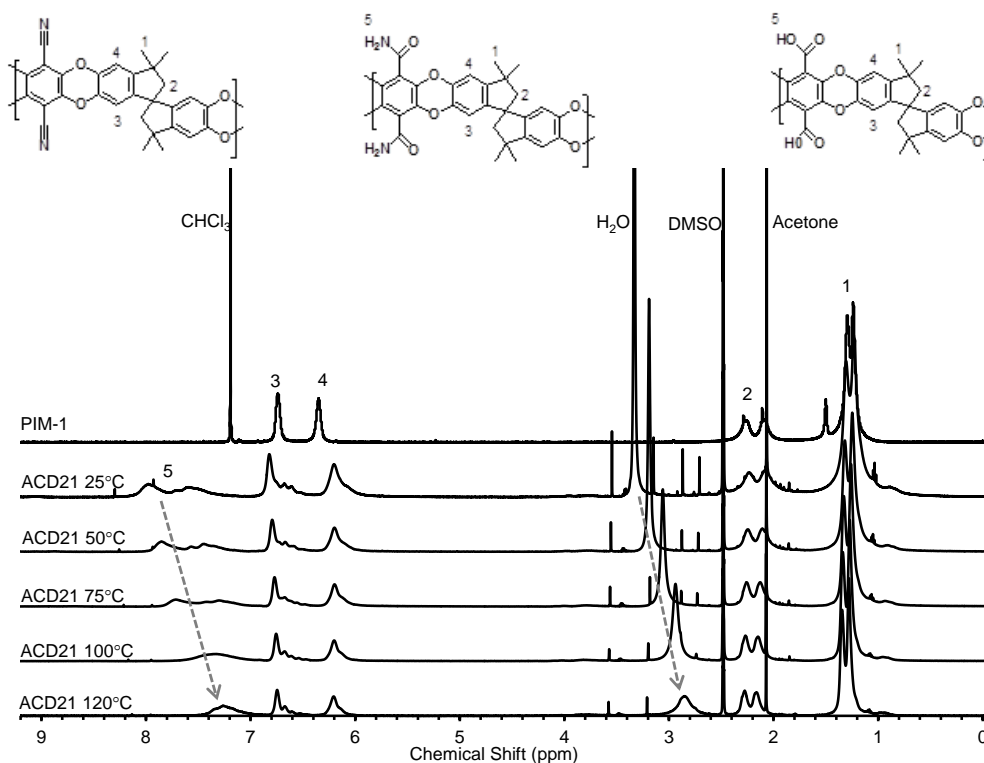
Fig. 4 ^{1}H NMR spectra of (from the top) PIM-1 in $CDCl_3$ at room temperature and ACD21 in d_6-DMSO at 25, 50, 75, 100 and 120°, showing peak assignments for PIM-1, amide and carboxylic acid structures. Grey dashed arrows indicate the shifts in peak 5 (due to amide or carboxylic acid protons) and the water peak with increasing temperature.

Extent of hydrolysis

Two independent methods, IR and UV, were used to determine the mole fraction of nitrile units, x_{CN}. Hence, the fraction of nitrile groups hydrolysed could be calculated as $(1-x_{CN})$, and the percentage hydrolysis as $100(1-x_{CN})$.

From IR, x_{CN} was calculated from the area under the CN peak at 2240 cm^{-1}, I_{CN}, and the area of the CH region at 2800–3010 cm^{-1}, I_{CH}, for the hydrolysed product and for the parent PIM-1, using Eqn. (2).

$$x_{CN} = \frac{\left(I_{CN}/I_{CH}\right)_{\text{Hydrolysed PIM}}}{\left(I_{CN}/I_{CH}\right)_{\text{PIM-1}}} \qquad (2)$$

Values of x_{CN} and percentage hydrolysis from IR are given in **Table 3**.

From UV, x_{CN} was calculated from the absorbances at wavelengths of 326, 384 and 444 nm (A_{326}, A_{384} and A_{444}, respectively), using Eqn. (3).

$$x_{CN} = \frac{A_{384}+A_{444}}{A_{326}+A_{384}+A_{444}} \qquad (3)$$

This assumes that the absorbances at 384 and 444 nm are associated with unconverted nitrile (in repeat units with one or two unconverted nitrile groups, respectively), and the absorbance at 326 nm is associated with converted groups, as discussed above. Average values of x_{CN} determined from UV spectra in DMAc and DMSO are included in **Table 3**. Values of percentage hydrolysis from UV are compared with those from IR in **Fig. 5**. Good agreement can be seen between the two techniques.

Table 3 Mole fractions of nitrile, x_{CN}, amide, x_{CONH2}, carboxylic acid, x_{COOH}, ammonium carboxylate, x_{COONH4}, and sodium carboxylate, x_{COONa}, in hydrolysis products, and percentage hydrolysed and percentage carboxylated.

Sample	x_{CN} (IR)	x_{CN} (UV)[a]	x_{CONH2}	x_{COOH}	x_{COONH4}	x_{COONa}	% Hydrolysed[b]	% Carboxylated
ACD1	0.16	0.20	0.77	0.02	0.05	–	84	7
ACD8	0.10	0.04	0.70	0.14	0.06	–	90	20
ACD14	0.08	0.06	0.62	0.19	0.11	–	92	30
ACD21	0.04	0.03	0.59	0.03	0.16	0.18	96	37
ACD23	0.02	0.03	0.48	0.04	0.07	0.40	98	51
AMD1	0.76	0.71	0.24[c]	–	–	–	24	–
AMD2	0.42	0.47	0.58[c]	–	–	–	58	–
AMD3	0.24	0.28	0.67	0.08	0.01	–	76	8
AMD7	0.11	0.11	0.78	0.07	0.04	–	89	11

[a]Average from UV in DMSO and DMAc [b]From IR [c]Assuming no carboxylation

Fig. 5 Comparison of percentage hydrolysis from UV and IR. The dashed line indicates equal values.

Composition of hydrolysis products

The analysis of composition is based on the assumption that up to five species may be present in the polymer structure: unconverted nitrile, amide, carboxylic acid, ammonium carboxylate and sodium carboxylate, with mole fractions x_{CN}, x_{CONH2}, x_{COOH}, x_{COONH4} and x_{COONa}, respectively. If no other structures are present, then the sum of these mole fractions is unity.

$$x_{CN} + x_{CONH2} + x_{COOH} + x_{COONH4} + x_{COONa} = 1 \qquad (4)$$

The mole fraction of nitrile, x_{CN}, may be determined from either IR spectroscopy (**Eqn. 2**) or UV spectroscopy (**Eqn. 3**), as discussed above. The IR method is arguably more reliable and the IR data are used in the analysis below.

^{1}H NMR spectroscopy enables x_{CONH2} to be calculated if x_{COOH} is known, or vice versa. Each repeat unit in the polymer contains four aromatic protons and two functional groups (either unconverted nitrile or one of the converted forms), thus there are two aromatic protons associated with each functional group. There are two carbonyl protons associated with an amide group, and one with a carboxylic acid group. Thus, the ratio of carbonyl to aromatic protons is

$$\frac{I_{CO-H}}{I_{Ar-H}} = \frac{2x_{CONH2} + x_{COOH}}{2} \qquad (5)$$

Hence

$$x_{CONH2} = \left(\frac{I_{CO-H}}{I_{Ar-H}}\right) - 0.5x_{COOH} \qquad (6)$$

Elemental analysis provides additional information that enables the composition of the hydrolysed products to be determined. It is necessary to convert from the experimentally determined weight percentages to the required mole fractions. Given that all repeat units have the same carbon content (29 carbon atoms per polymer repeat unit and thus 14.5 carbon atoms per functional group), we can make use of the weight ratios of sodium to carbon, wt%Na/wt%C, and of nitrogen to carbon,

wt%N/wt%C. The mole ratios of sodium to carbon, N_{Na}/N_C, and of nitrogen to carbon, N_N/N_C, are given by

$$\frac{N_{Na}}{N_C} = \frac{x_{COONa}}{14.5} = \frac{wt\%Na}{wt\%C} \frac{M_C}{M_{Na}} \qquad (7)$$

and

$$\frac{N_N}{N_C} = \frac{x_{CN} + x_{CONH2} + x_{COONH4}}{14.5} = \frac{wt\%N}{wt\%C} \frac{M_C}{M_N} \qquad (8)$$

where M_C, M_{Na} and M_N are the atomic masses of C, Na and N, respectively (i.e., $M_C = 12.011$, $M_{Na} = 22.99$, $M_N = 14.007$).

The mole fraction of sodium carboxylate, x_{COONa}, is determined using **Eqn. 7** and the sum of the mole fractions of nitrogen-containing groups, $x_{CN} + x_{CONH2} + x_{COONH4}$, using **Eqn. 8**. The mole fraction of carboxylic acid, x_{COOH}, is then calculated using **Eqn. 4**. Hence the mole fraction of amide, x_{CONH2}, is obtained from **Eqn. 6**, which enables the mole fraction of ammonium carboxylate, x_{COONH4}, to be determined using **Eqn. 4**.

Compositions calculated in this way are given in **Table 3**. A full analysis could not be carried out for samples with low degrees of hydrolysis (AMD1, AMD2), which were only partially soluble in DMSO at the concentrations required for NMR, but these may be assumed to be minimally carboxylated. Included in **Table 3** are values of percentage carboxylated, determined as $100(x_{COOH} + x_{COONH4} + x_{COONa})$. The highest extent of carboxylation achieved was 51% (for ACD23), although the extent of hydrolysis for this sample was 98%, *i.e.*, even the most fully converted sample was almost half amide. It is likely that hydrolysed products previously reported in the literature as "carboxylated" in reality had a significant amide content.

Contact angle

Water contact angles are given in **Table 4**, and are plotted against percentage hydrolysed in **Fig. 6**. As would be expected, on hydrolysis the polymer surface became more hydrophilic, the contact angle decreasing from 85° for PIM-1 to about 60° for the most fully hydrolysed samples.

Table 4: Water contact angles, BET surface areas and uptakes of the dyes Safranin O and Orange II from aqueous solution, for PIM-1 and for hydrolysis products.

Sample	Contact angle (degrees)	BET surface area ($m^2 \, g^{-1}$)	Safranin O uptake ($mg \, g^{-1}$)	Orange II uptake ($mg \, g^{-1}$)
PIM-1	85.3±2.0	750	15	11
ACD1	68±3.5	675	100	35
ACD8	65.7±2.4	396	154	25
ACD14	–	–	156	26
ACD21	60±3.4	207	214	21
ACD23	–	265	467	9
AMD1	76.1±5.8	552	54	43
AMD2	71.5±5.2	499	65	35
AMD3	67.5±1.2	429	80	33
AMD7	60.8±3.3	418	81	33
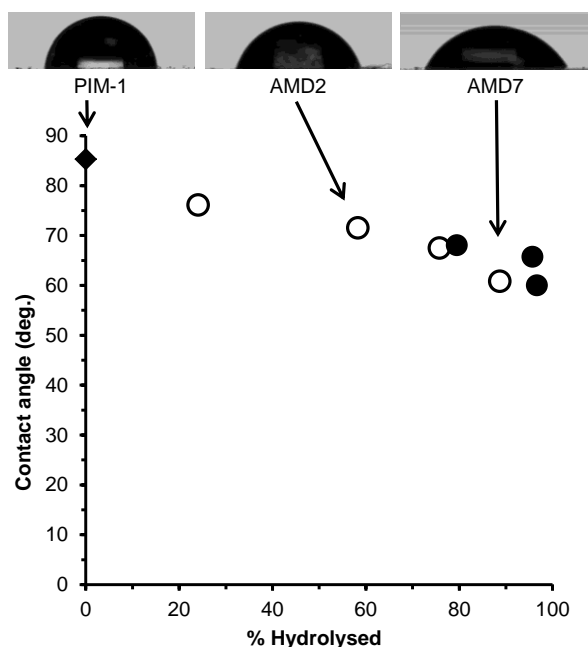
Fig. 6 Photographs of water drops on surfaces of PIM-1, AMD2 and AMD7, and dependence of water contact angle on percentage hydrolysed, showing data for PIM-1 (◆), samples hydrolysed at 120°C with 20% NaOH (●) and samples hydrolysed at 100°C with 10% NaOH (○).

N₂ adsorption

BET surface areas determined from N_2 adsorption data at −196 °C, are given in **Table 4** and plotted against the time of the hydrolysis reaction in **Fig. 7**. Hydrolysis led to a reduction in apparent surface area, as has previously been discussed.[18] This can be attributed to hydrogen-bonding interactions, which create a tighter structure, leading to reduced uptake and slower adsorption kinetics.
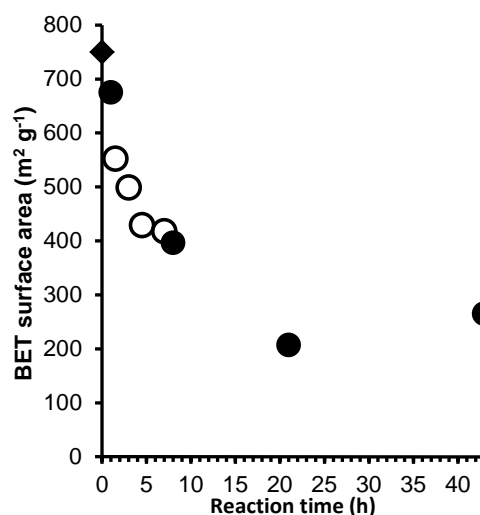
Fig. 7 BET surface area versus reaction time for samples hydrolysed at 120°C with 20% NaOH (●) and 100°C with 10% NaOH (○), and data for PIM-1 (◆).

Thermogravimetric analysis

TGA curves for samples hydrolysed at 120°C with 20% NaOH (ACD series) and at 100°C with 10% NaOH (AMD series) are compared with the parent polymer, PIM-1, in **Figs. 8a** and **8b**, respectively. PIM-1 shows little weight loss below 460°C. Hydrolysed products show lower temperature weight losses. Weight losses below 150°C may be attributed to adsorbed moisture and volatile organics. For the hydrolysis products, weight losses in the range 150–280°C appear to be related to the proportion of carboxylate salt (ammonium and sodium) in the polymer (**Fig. 8c**), while weight losses in the range 280–460°C may be linked, at least in part, to the proportion of amide in the polymer (**Fig. 8d**).
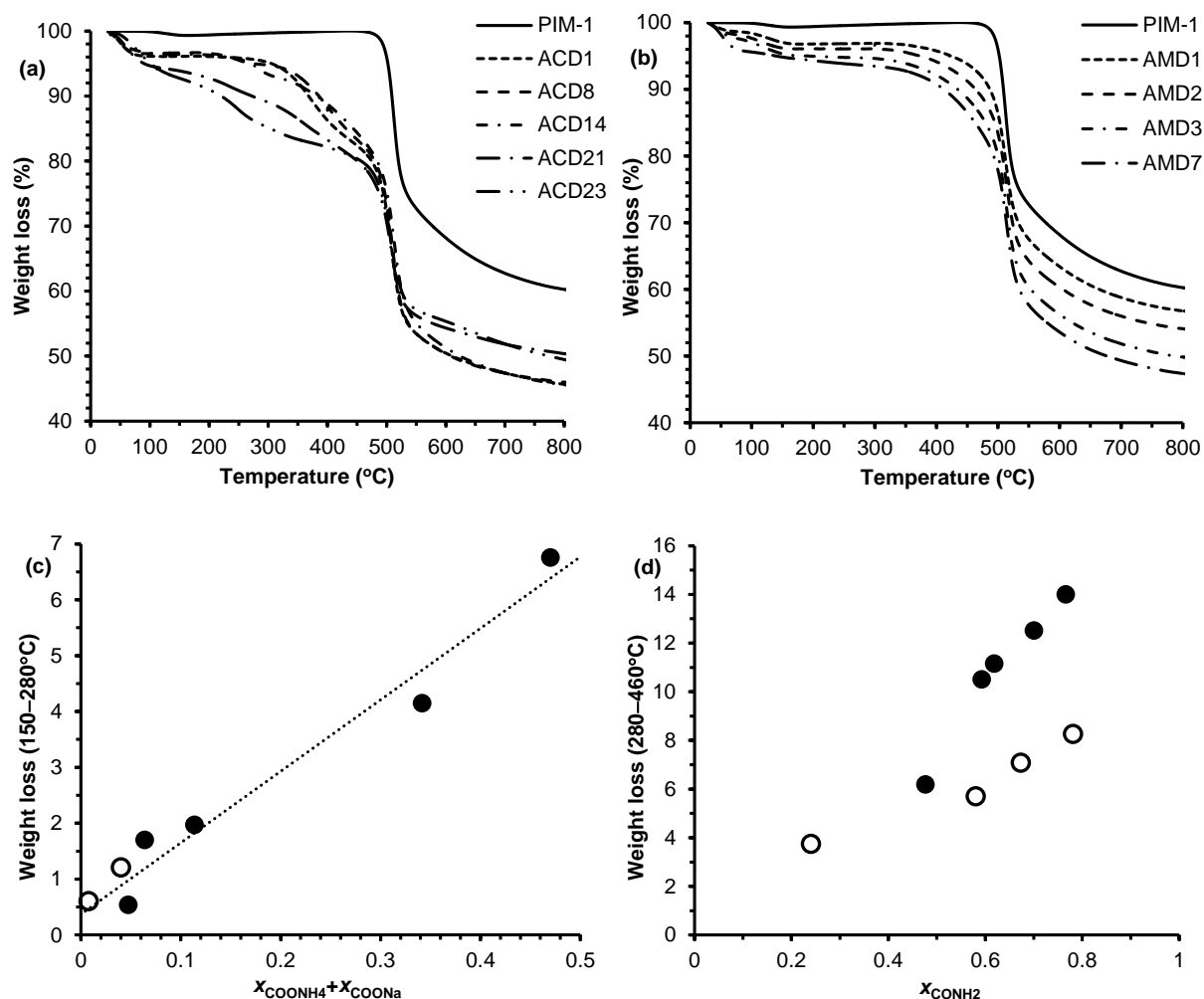
Fig. 8. TGA curves for samples hydrolysed at **(a)** 120°C with 20% NaOH and **(b)** 100°C with 10% NaOH, and comparison to PIM-1 in each case. For ACD samples (●) and AMD samples (○), **(c)** dependence of weight loss in the temperature range 150–280°C on the mole fraction of ammonium and sodium carboxylate structures in the polymer (the dashed line is a guide to the eye) and **(d)** dependence of weight loss in the temperature range 280–460°C on the mole fraction of amide in the polymer.

Dye adsorption

Mass uptakes of the cationic dye Safranin O (**Fig. 1b**) and the anionic dye Orange II (**Fig. 1c**) from aqueous solution by PIM-1 and hydrolysed products are given in **Table 4**. The hydrolysed products all showed higher affinities for Safranin O than the parent polymer, with the amount adsorbed increasing with increasing percentage carboxylated, as seen in **Fig. 9**. The most highly carboxylated sample (ACD23) exhibited 31 times the uptake of the parent polymer. In contrast, uptake of Orange II, while higher for most of the hydrolysis products than for PIM-1, decreased with increasing percentage carboxylated (**Fig. 9**), and the most highly carboxylated sample showed marginally lower uptake than the parent polymer.
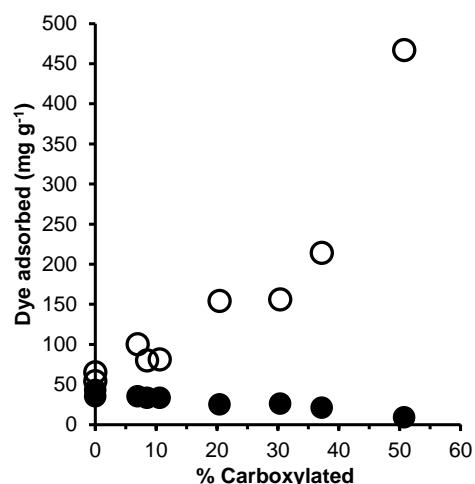
Fig. 9 Dependence of the amounts adsorbed from aqueous solution of Safranin O (○) and Orange II (●) on the percentage of carboxylated groups (COOH, $COONH_4$ and COONa) in the hydrolysis products.

Conclusions

Depending on the reaction conditions and washing procedures, base-catalysed hydrolysis of PIM-1 may generate products with a mixture of amide, carboxylic acid, ammonium carboxylate and sodium carboxylate structures. No single characterization method enables amide to be distinguished unambiguously from carboxylated PIM-1. However, by combining data from IR or UV with ^{1}H NMR and elemental analysis, compositions may be determined. Even the most fully hydrolysed samples retain a significant proportion of amide, together with carboxylated structures, and most products are more than half amide. As might be expected, with increasing degree of hydrolysis the polymer becomes more hydrophilic, the water contact angle decreasing from 85° for the parent polymer PIM-1 to about 60° for highly hydrolysed samples. Hydrolysis also reduces the apparent surface area of the polymer as determined by low temperature nitrogen adsorption.

The ability to tailor the composition, and therefore the properties of the polymer, is of relevance to a variety of separation processes. This was demonstrated for the adsorption of dyes from aqueous solution. Most hydrolysis products showed enhanced adsorption of ionic dyes, compared to the parent polymer, with the selectivity depending markedly on the composition of the polymer. Uptake of a cationic dye increased dramatically with increasing degree of carboxylation, while uptake of an anionic dye decreased.

Notes and references

[a] School of Chemistry, University of Manchester, Manchester, M13 9PL, UK. Email: Peter.Budd@manchester.ac.uk.

Acknowledgement

References

1. P. M. Budd, B. S. Ghanem, S. Makhseed, N. B. McKeown, K. J. Msayib and C. E. Tattershall, *Chem. Commun.*, 2004, 230-231.
2. N. B. McKeown and P. M. Budd, *Macromolecules*, 2010, **43**, 5163-5176.
3. P. M. Budd, E. S. Elabas, B. S. Ghanem, S. Makhseed, N. B. McKeown, K. J. Msayib, C. E. Tattershall and D. Wang, *Adv. Mater.*, 2004, **16**, 456-459.
4. P. M. Budd, K. J. Msayib, C. E. Tattershall, B. S. Ghanem, K. J. Reynolds, N. B. McKeown and D. Fritsch, *J. Membr. Sci.*, 2005, **251**, 263-269.
5. P. M. Budd, N. B. McKeown, B. S. Ghanem, K. J. Msayib, D. Fritsch, L. Starannikova, N. Belov, O. Sanfirova, Y. Yampolskii and V. Shantarovich, *J. Membr. Sci.*, 2008, **325**, 851-860.
6. P. M. Budd and N. B. McKeown, *Polym. Chem.*, 2010, **1**, 63-68.
7. D. Fritsch, P. Merten, K. Heinrich, M. Lazar and M. Priske, *J. Membr. Sci.*, 2012, **401-402**, 222-231.
8. P. Li, T. S. Chung and D. R. Paul, *J. Membr. Sci.*, 2013, **432**, 50-57.
9. S. Tsarkov, V. Khotimskiy, P. M. Budd, V. Volkov, J. Kukushkina and A. Volkov, *J. Membr. Sci.*, 2012, **423-424**, 65-72.
10. A. V. Maffei, P. M. Budd and N. B. McKeown, *Langmuir*, 2006, **22**, 4225-4229.
11. C. A. Jeffs, M. W. Smith, C. A. Stone, C. G. Bezzu, K. J. Msayib, N. B. McKeown and S. P. Perera, *Micropor. Mesopor. Mater.*, 2013, **170**, 105-112.
12. N. A. Rakow, M. S. Wendland, J. E. Trend, R. J. Poirier, D. M. Paolucci, S. P. Maki, C. S. Lyons and M. J. Swierczek, *Langmuir*, 2010, **26**, 3767-3770.
13. J. Christopher Thomas, J. E. Trend, N. A. Rakow, M. S. Wendland, R. J. Poirier and D. M. Paolucci, *Sensors*, 2011, **11**, 3267-3280.
14. S. T. Hobson, S. Cemalovic and S. V. Patel, *Analyst*, 2012, **137**, 1284-1289.
15. H. J. Mackintosh, P. M. Budd and N. B. McKeown, *J. Mater. Chem.*, 2008, **18**, 573-578.
16. S. Makhseed, F. Al-Kharafi, J. Samuel and B. Ateya, *Catalysis Commun.*, 2009, **10**, 1284-1287.
17. N. Du, G. P. Robertson, J. Song, I. Pinnau and M. D. Guiver, *Macromolecules*, 2009, **42**, 6038-6043.
18. J. Weber, N. Du and M. D. Guiver, *Macromolecules*, 2011, **44**, 1763-1767.
19. N. Du, M. M. Dal-Cin, G. P. Robertson and M. D. Guiver, *Macromolecules*, 2012, **45**, 5134-5139.
20. W. F. Yong, F. Y. Li, T. S. Chung and Y. W. Tong, *J. Membr. Sci.*, 2014, **462**, 119-130.
21. N. Du, H. B. Park, G. P. Robertson, M. M. Dal-Cin, T. Visser, L. Scoles and M. D. Guiver, *Nature Mater.*, 2011, **10**, 372-375.
22. J. K. Moore, M. D. Guiver, N. Du, S. E. Hayes and M. S. Conradi, *J. Phys. Chem. C*, 2013, **117**, 22995-22999.
23. N. Du, G. P. Robertson, M. M. Dal-Cin, L. Scoles and M. D. Guiver, *Polymer*, 2012, **53**, 4367-4372.
24. C. R. Mason, L. Maynard-Atem, N. M. Al-Harbi, P. M. Budd, P. Bernardo, F. Bazzarelli, G. Clarizia and J. C. Jansen, *Macromolecules*, 2011, **44**, 6471-6479.
25. H. A. Patel and C. T. Yavuz, *Chem. Commun.*, 2012, **48**, 9989-9991.
26. R. Swaidan, B. S. Ghanem, E. Litwiller and I. Pinnau, *J. Membr. Sci.*, 2014, **457**, 95-102.
27. C. R. Mason, L. Maynard-Atem, K. W. J. Heard, B. Satilmis, P. M. Budd, K. Friess, M. Lanc, P. Bernardo, G. Clarizia and J. C. Jansen, *Macromolecules*, 2014, **47**, 1021-1029.
28. B. G. Kim, D. Henkensmeier, H.-J. Kim, J. H. Jang, S. W. Nam and T.-H. Lim, *Macromol. Res.*, 2014, **22**, 92-98.
29. N. Du, M. M. Dal-Cin, I. Pinnau, A. Nicalek, G. P. Robertson and M. D. Guiver, *Macromol. Rapid Commun.*, 2011, **32**, 631-636.
30. M. M. Khan, G. Bengtson, S. Shishatskiy, B. N. Gacal, M. Mushfequr Rahman, S. Neumann, V. Filiz and V. Abetz, *Eur. Polym. J.*, 2013, **49**, 4157-4166.
31. J. McMurry, *Organic Chemistry*, Thomson Brooks/Cole, Belmont, CA, 2004.
32. T. N. Sorrell, *Organic Chemistry*, University Science Books, Sausalito, CA, 1997.

RSC Advances Accepted Manuscript

33. O. Sanli, *Eur. Polym. J.*, 1990, **26**, 9-13.
34. A. D. Litmanovich and N. A. Plate, *Macromol. Chem. Phys.*, 2000, **201**, 2176-2180.
35. V. A. Dyatlov, T. A. Grebeneva, I. R. Rustamov, A. A. Koledenkov, N. V. Kolotilova, V. V. Kireev and B. M. Prudskov, *Polymer Science, Series B*, 2012, **54**, 161-166.

RSC Advances Accepted Manuscript